Global Change Biology

Global Change Biology (2012) **18**, 385–399, doi: 10.1111/j.1365-2486.2011.02536.x

TECHNICAL ADVANCE

Calculating CO_2 and H_2O eddy covariance fluxes from an enclosed gas analyzer using an instantaneous mixing ratio

GEORGE BURBA*, ANDRES SCHMIDT†, RUSSELL L. SCOTT‡, TARO NAKAI§, JAMES KATHILANKAL*, GERARDO FRATINI*, CHAD HANSON†, BEVERLY LAW†, DAYLE K. MCDERMITT*, ROBERT ECKLES*, MICHAEL FURTAW* and MICHAEL VELGERSDYK*

*LI-COR Biosciences, 4421 Superior Street, Lincoln, NE 68504, USA, †College of Forestry, Oregon State University, 328 Richardson Hall, Corvallis, OR 97331, USA, ‡Agricultural Research Service, USDA, 2000 E. Allen Road, Tucson, AZ 85719, USA, §International Arctic Research Center, University of Alaska, 930 Koyukuk Drive, Fairbanks, AK 99775, USA

Abstract

Eddy covariance flux research has relied on open- or closed-path gas analyzers for producing estimates of net ecosystem exchange of carbon dioxide (CO_2) and water vapor (H_2O). The two instruments have had different challenges that have led to development of an enclosed design that is intended to maximize strengths and minimize weaknesses of both traditional designs. Similar to the closed-path analyzer, the enclosed design leads to minimal data loss during precipitation events and icing, and it does not have surface heating issues. Similar to the open-path design, the enclosed design has good frequency response due to small flux attenuation loss in the short intake tube, does not need frequent calibration, has minimal maintenance requirements, and can be used in a very low power configuration. Another important feature of such a design is the ability to output instantaneous mixing ratio, or dry mole fraction, so that instantaneous thermal and pressure-related expansion and contraction, and water dilution of the sampled air have been accounted for. Thus, no density corrections should be required to compute fluxes during post-processing. Calculations of CO_2 and H_2O fluxes via instantaneous mixing ratio from the new enclosed CO_2/H_2O gas analyzer were tested in nine field experiments during 2009–2010 in a wide range of ecosystems and setups. Fluxes computed via a mixing ratio output from the instrument without applying density corrections were compared to those computed the traditional way using density corrections. The results suggest that with proper temperature, water vapor, and pressure measurements in the cell, gas fluxes can be computed confidently from raw covariance of mixing ratio and vertical wind speed, multiplied by a frequency response correction. This has important implications for future flux measurements, because avoiding hourly density corrections could have the advantages of increasing flux measurement quality and temporal resolution, reducing the magnitude of minimum detectable flux, unifying data processing steps, and assuring better intercomparison between different sites and networks.

Keywords: carbon dioxide exchange, closed path, CO_2 flux, density correction, eddy covariance, enclosed analyzer, flux, gas analyzer, H_2O flux, mixing ratio, open path, WPL

Received 6 May 2011; revised version received 5 August 2011 and accepted 15 August 2011

Introduction

Traditionally, high-speed gas analyzers with response rate of 10 Hz or higher utilized for measurements of eddy covariance fluxes of carbon dioxide (CO_2) and water vapor (H_2O) are designed in one of two configurations; open path or closed path. Both designs are well known, firmly established, and widely used in flux measurement research to understand the net exchange of CO_2 and H_2O between terrestrial ecosystems and the atmosphere (Leuning & Judd, 1996; Massman *et al*., 2004; Law, 2006). The advantages and deficiencies of each design are also well known.

Correspondence: George Burba, tel. + 1 402 467 0608, fax + 1 402 467 2819, e-mail: george.burba@licor.com

Closed-path analyzers able to gather data during precipitation events, can often be climate-controlled, and are not subject to surface heating issues (Burba *et al*., 2008; Clement *et al*., 2009; Jarvi *et al*., 2009). However, they are associated with significant frequency loss in long intake tubes, especially affecting H_2O flux, due to sorption and desorption of water molecules on the tubing walls (Lenschow & Raupach, 1991; Massman & Ibrom, 2008). They may also require relatively frequent calibrations, and may need a high power pump, leading to greater power consumption; a significant challenge for remote locations.

Open-path analyzers have good frequency response for both CO_2 and H_2O, usually exhibit long-term stability, and have low or moderate sensitivity to window contamination. They do not require pumps, have low

power demand, and do not need frequent calibrations. However, data collected during precipitation events and icing are often unusable (Clement *et al*., 2009), and may require a correction for instrument surface heating in very cold conditions (Grelle & Burba, 2007; Burba *et al*., 2008; Jarvi *et al*., 2009).

A new enclosed gas analyzer, the LI-7200 (LI-COR Biosciences, Lincoln, NE, USA), field tested during 2005–2009 and widely deployed in flux research starting in 2009, is a combination of the traditional open-path and closed-path designs (Clement *et al*., 2009; Burba *et al*., 2010). Although mechanically similar to the traditional long-tube closed-path design, the enclosed design is a low power solution with a short intake tube. This design is intended to solve most of the issues of the two traditional designs without sacrificing their positive attributes, maximizing their strengths and minimizing weaknesses.

Analogous to the closed-path solution, the enclosed design results in minimal data loss due to precipitation and icing, and is not subject to surface heating phenomena (Burba *et al*., 2008; Clement *et al*., 2009). Analogous to the open-path solution, the enclosed design leads to a good frequency response because of the short intake tube, does not require frequent calibrations, and operates with low power consumption. Further details on the characteristics of the enclosed design can be found in Burba *et al*. (2010).

Another important feature of an enclosed design is the ability to output instantaneous mixing ratio, or dry mole fraction, because native density measurements can be converted to mixing ratio units using instantaneous measurements of temperature, water vapor, and pressure inside the sampling cell. Outputting instantaneous mixing ratios implies that the instantaneous thermal and pressure-related expansion and water dilution of the sampled air have been accounted for in such a conversion (Leuning, 2004; Nakai *et al*., 2011). Thus, density corrections are not required to compute fluxes when the instantaneous mixing ratio is used.

This method of calculating fluxes has been frequently used with traditional closed-path analyzers (e.g., LI-COR LI-6262 and LI-7000), because instantaneous fluctuations in the air temperature of the sample were attenuated in the long intake tube; instantaneous pressure fluctuations were assumed negligible; H_2O was measured simultaneously with CO_2, and dry mole fraction was output. In an enclosed design with a short tube, most, but not all, of the instantaneous temperature fluctuations are attenuated, thus calculating fluxes using the mixing ratio output of this type of instrument requires validation.

Fluxes of CO_2 and H_2O from nine field deployments of the new enclosed analyzer in various ecosystems and setups were examined in this study. The experiments consisted of seven deployments of the AmeriFlux Roving Intercomparison System in California, Arizona, New Mexico, and Oregon; one deployment at a USDA flux site in Arizona; one deployment at the University of Alaska Fairbanks (UAF) site, and one deployment at the LI-COR test facility in Lincoln, Nebraska. Fluxes were computed in two ways: (i) in the traditional way, using gas density output with subsequent density corrections during postprocessing after Webb *et al*. (1980), and (ii) using a mixing ratio output from the instrument without applying density corrections.

The focus of this study was on the following key aspects of the traditional and mixing ratio-based flux measurements by an enclosed analyzer, and related calculations inside the instrument and during postprocessing.

1 Degree of temperature attenuation by the short intake tube, and its implications for traditional and mixing ratio flux calculations.
2 Pressure drop and instantaneous pressure fluctuations in the cell, and their implications for traditional and mixing ratio flux calculations.
3 Validation of instantaneous mixing ratio computed in real time inside the instrument vs. hand calculations during postprocessing.
4 Comparison of traditionally computed hourly fluxes of CO_2 and H_2O following Webb *et al*. (1980), with those computed using mixing ratio across the sampled ecosystems and setups.
5 Feasibility and implications of computing fluxes from the mixing ratio output by an enclosed analyzer.

Materials and methods

Theoretical considerations

Fundamentally, fluxes can be computed from a covariance between vertical wind speed and gas content following (Webb *et al*., 1980; Leuning, 2004; Massman, 2004):

$$F_{cm} = \overline{w\rho s_w} \approx \overline{\rho_d}\ \overline{w's'}, \tag{1}$$

where F_{cm} is final corrected flux computed using mixing ratio; w is vertical wind speed; ρ is total air density; s_w is wet mole fraction; ρ_d is dry air density; s is mixing ratio (dry mole fraction). The overbar indicates mean quantity, and the prime symbol indicates instantaneous deviation from the mean.

However, traditional flux calculations usually use density measurements native to the light absorption-based gas analyzers, and then apply density corrections after Webb *et al*. (1980), hereafter referred to as WPL:

$$F_{ct} = \overline{w'q_c'} + \mu\frac{E}{\overline{\rho_d}}\frac{\overline{q}_c}{1+\mu(\overline{\rho_v}/\overline{\rho_d})} + \frac{H}{\overline{\rho}C_p}\frac{\overline{q_c}}{\overline{T}} + 0, \tag{2}$$

where F_{ct} is the final WPL-corrected flux, computed in the traditional manner using gas density q_c; E is evapotranspiration;

H is sensible heat flux; ρ_v is H_2O vapor density; C_p is specific heat of air; T is sampled air temperature in K; μ is a ratio of molar masses of air to water (μ = 1.6077).

The first term on the right-hand side of Eqn (2) is a raw flux covariance. The second term is a water vapor dilution term (*LE*-term), where E is computed from H_2O density measured in the cell of an analyzer simultaneously with CO_2. The third term is a thermal expansion and contraction (*H*-term), where H in the cell is reduced in the enclosed analyzer by 90–99% of ambient, due to attenuation by an intake tube (Clement *et al*., 2009; Burba *et al*., 2010), and is dependent on flow rate, ambient sensible heat flux, surface roughness, thermal stability, and instrument height. The remainder is computed from instantaneous temperature measurements inside the cell. This term is usually neglected in closed-path analyzers with long intake tubes, but should not necessarily be discarded in the short-tube enclosed design.

The fourth and last term is a pressure expansion (*P*-term), which is usually assumed to be negligible. However, it may be non-negligible in some situations, especially when measuring in fluctuating pressure fields (Lee & Massman, 2011; Nakai *et al*., 2011; Zhang *et al*., 2011), and may be computed from the gas pressure in the cell, p, after Lee & Massman (2011):

$$P\text{-term} = -\overline{q_c}\left(1 + \mu\frac{\overline{\rho_v}}{\overline{\rho_d}}\right)\frac{\overline{w'p'}}{\overline{p}}. \quad (3)$$

An enclosed analyzer can utilize Eqn (1) for flux calculations because it measures instantaneous temperature and pressure in the cell alongside the gas density and water vapor. The mixing ratio, s, expressed as moles of gas or water vapor per moles of dry air, can be computed in an enclosed analyzer in real time from the gas density measurements as follows:

$$S = \frac{S_w}{1 - X_w} = \frac{q_c(RT/p)}{1 - X_w}, \quad (4)$$

where X_w is instantaneous water mole fraction in the cell, T is instantaneous sampled air temperature in the cell, and R is a gas constant.

Precise time matching between q_c, T, p, and X_w is extremely important for computing correct instantaneous s, because temperature- and pressure-related expansions and contractions, and water vapor dilution are instantaneous processes affecting q_c. Therefore, special care should be taken in the analyzer software to properly measure, delay, and align all inputs in Eqn (4), as described below in the Instrument design. The Results and discussion also includes a comparison of real-time calculations of s by the analyzer software with manual calculations from raw instantaneous time series of each of the components in Eqn (4) during postprocessing.

Several novel approaches were recently proposed for the order of the corrections in eddy covariance flux calculations (Ibrom *et al*., 2007), for the importance of including the pressure term into WPL computations (Lee & Massman, 2011; Nakai *et al*., 2011; Zhang *et al*., 2011), and for the form of the original Webb–Pearman–Leuning correction (Liu, 2005, 2006, 2009; Kowalski, 2006; Leuning, 2007; Lee & Massman, 2011). These are important developments in eddy covariance flux methodology, but comparing and testing these approaches fall outside the scope of this study. The focus of this study is, rather, on comparing mixing ratio-based gas flux calculations to those from a widely used traditional approach. Therefore, for density-based flux calculations, Eqn (2) is used as shown, and co-spectral frequency response corrections (Kaimal *et al*., 1972; Moore, 1986; Massman, 2000; Massman, 2001) are applied to the raw flux covariance (Massman, 2004).

Similar frequency response corrections were applied to the mixing ratio-based flux covariance. This is not an ideal procedure, because mixing ratio does not have the influence of fluctuating temperature, pressure, and water vapor built into its final value. However, theoretical co-spectral corrections for mixing ratio *per se* have not yet been developed, to our knowledge. Frequency corrections for both density-based and mixing ratio-based fluxes have been verified by comparing the area under the actual co-spectral shape of $w'q_c'$ and $w's'$ with the area under the Kaimal and $w'T'$ co-spectra.

Instrument design

The LI-7200 is an enclosed gas analyzer enabled for operation with a short intake tube. Instantaneous air temperature and air pressure are measured inside the sampling cell, along with instantaneous measurements of CO_2 and H_2O concentrations. When used with a long tube (>1.5–2 m), the analyzer functions as a closed-path device. When used with an extremely short tube (ca. 0–0.5 m), it behaves more closely to an open-path device. When used in its default configuration (with a 0.5–1.5 m tube), it has characteristics of both designs. Table 1 outlines subtle but important differences between the three designs. Optimum tube lengths for different applications are discussed in Clement *et al*. (2009) and Burba *et al*. (2010).

The design of the analyzer is based on the optical technology of the open-path LI-7500 analyzer (LI-COR Inc, 2001), with some improvements and modifications (Clement *et al*., 2009; Burba *et al*., 2010). The enclosed analyzer outputs instantaneous gas density used in traditional flux calculations (Webb *et al*., 1980). It also outputs instantaneous mixing ratio of CO_2 and H_2O, corrected for dilution, and thermal and pressure expansion using instantaneous water, temperature and pressure measurements inside the cell, so that no WPL terms are required during postprocessing.

Instantaneous temperatures are measured just before air enters the sampling volume and immediately after air leaves the sampling volume. Instantaneous pressure is measured in the middle of the cell with a high speed, high precision differential pressure sensor combined with a low speed, high precision absolute pressure sensor located in the electronic box. Further details of the design and the traditional density-based performance of the analyzer are described in detail in Burba *et al*. (2010) and in the instrument manual (LI-COR, Inc, 2010).

As mentioned in Theoretical Considerations, precise time matching between q_c, T, p, and X_w is extremely important for computing correct instantaneous s in real time using Eqn (4). Therefore, special attention was given in the analyzer software to properly measure, delay, and align all inputs required for Eqn (4). In this particular design, instantaneous air temperatures measured near the inlet (T_{in}) and outlet (T_{out}) of the sam-

Table 1 Typical implementation and key practical features of open-path, closed-path, and enclosed designs of fast gas analyzers used in eddy covariance flux measurements

	Open-path design	Enclosed design	Closed-path design
Sampling cell position	Next to the sonic anemometer	Within 1.5 m from the sonic anemometer	Away from the sonic anemometer
Intake tube length	None	Few centimeters to 1.5 m	4.0–40.0 m or more
Fast T and p in the cell	No	Yes	No, in pre-2010 models
Frequency losses	Sensor separation, flow disturbance, path averaging	Small frequency dampening, path averaging	Medium-to-large frequency dampening, path averaging
Temperature attenuation	None	On average, 90–99%	On average, over 90–99%
WPL size	Large	Small, mostly *LE*-term	Small, mostly *LE*-term
Ability to output mixing ratio	None	Yes	Yes, assuming zero or measured T' and p'
Cell cleaning	Easy, user cleanable	Easy, user cleanable	Moderate-to-hard, often not user cleanable
Loss during precipitation	Large	Limited by anemometer	Limited by anemometer
Calibration, zero check	Weekly-to-monthly, manual	Weekly-to-monthly, manual or automated	Weekly-to-monthly, manual or automated

pling cell are weighted 1 : 4 to compute T in such a way that it properly reflects the temperature integrated over the entire cell volume for flow rates ranging from 12 to 17 lpm. The importance of proper weighting of T_{in} and T_{out} to characterize the high-speed temperature and mixing ratio of the air sample in an enclosed gas analyzer is illustrated in Table 2 by comparison with the closed-path standard. Furthermore, the outlet air temperature in the enclosed sampling cell is delayed in time in relation to the inlet cell temperature to describe the same air parcel, and all other signals are delayed in relation to T to compensate for the thermal inertia of thermocouples measuring inlet and outlet temperatures. Further details on the configuration and operation of this device can be found in the respective instruction manual (LI-COR, Inc, 2010) and in Burba *et al*. (2010).

Field experiments

To characterize the traditional aspects of the instrument performance, data from extensive field tests of the enclosed analyzer conducted during 2006–2009 over ryegrass in Nebraska and over a sawgrass wetland in Florida were used. In these experiments, the main focus was on instantaneous gas density, frequency response, and the magnitudes of density-based fluxes from the enclosed analyzer in comparison with the established open-path and closed-path standards. Temperature and pressure in the cell, data loss during precipitation, tube optimization, and power requirements were also examined. The results are provided in Burba *et al*. (2010). At the time of these experiments, automated real-time mixing ratio calculations were not yet available in the instrument software. However, various configurations, settings, and regiments provided a variety of conditions useful for examining temperature and pressure behavior in the cell. Here, we use the data from these experiments for evaluating temperature attenuation and magnitudes of the *H*-term in the cell, and instantaneous pressure and the *P*-term in the cell.

For comparison of mixing ratio-based flux calculations to the density-based flux calculations, data were used from a total of nine field experiments conducted during 2009–2010. These experiments covered a broad range of setups and conditions: six experiments from the AmeriFlux Roving Station utilizing the enclosed analyzer as a part of the AmeriFlux Quality Assurance and Quality Control Intercomparisons; one experiment from a USDA site in Arizona (AZ-2); one experiment from the UAF site (Nakai *et al*., 2011); and one experi-

Table 2 Illustration of the importance of proper weighting of T_{in} and T_{out} to characterize the high-speed temperature and mixing ratio of the air sample in an enclosed gas analyzer

Regiment	Slope	Offset (mmol m^{-2} s^{-1})	R^2
Using just T_{in} and ignoring T_{out}	0.94^{s}	0.00021	0.96
Using just T_{out} and ignoring T_{in}	1.02^{s}	0.00007	0.96
Arithmetic average of T_{in} and T_{out}	0.98^{s}	0.00014	0.96
Weighted average (1 : 4 for T_{in}:T_{out})	1.00	0.00010	0.96

Comparison of CO_2 fluxes from an enclosed gas analyzer with a closed-path reference: [fluxes from an enclosed gas analyzer] = [slope] × [fluxes from closed-path reference] + [offset], n = 774. The LI-7000 was used as a closed-path reference in the 2007 experiment in Lincoln, NE, described in Burba *et al*. (2010). Here and in all further superscript '*s*' indicates slopes that are significantly different from 1.

ment from the LI-COR field test facility in Lincoln, Nebraska (Burba *et al.*, 2010). The experiments covered a variety of ecosystems, from a semiarid shrubland in southern Arizona to a forest in central Alaska. Elevations above sea level ranged between 70 and 1593 m, and average temperatures ranged between 7.9 and 28.3 °C. Canopy height ranged from 0.1 to 30 m. The time of year was variable, and covered periods from March through November.

In all nine experiments, data were collected at 10 Hz, using a default 1-m intake tube with rain cup and insect screen, and without an external fine-particle filter. The default 14–15 lpm flow rate was used to sample the air. The inlet was installed next to a sonic anemometer with a sensor separation ranging from 0.10 to 0.25 m. The instrument placement height ranged from 2.5 to 48.0 m above the ground. Table 3 summarizes the site description for these experiments.

Most of the mixing ratio-based flux experiments in this study started recently, were relatively short in duration, ranging from weeks to a few months, and were primarily focused on hourly fluxes. These do not allow examining long-term effects on flux integration for all nine sites. Therefore, the focus of this study is on hourly mixing ratio-based fluxes compared to traditional density-based fluxes at nine different sites. Integrated effects over a longer time scale are studied for a single AK site in Nakai *et al.* (2011).

Data processing and quality control

In all experiments, eddy covariance flux data have undergone careful postprocessing, selection, and quality control. Postprocessing was nearly identical for density-based and mixing-ratio-based fluxes, and included standard steps to compute results from the instantaneous 10 Hz data: de-spiking, rotation, time delay computation in relation to vertical wind speed, standard frequency response corrections, stationarity tests, etc. These and other quality control steps were performed, generally following the FluxNet guidelines (Aubinet *et al.*, 1999; Foken *et al.*, 2004). Then, to assure proper comparison between results obtained with traditional density-based flux calculations and proposed mixing-ratio-based flux calculations, data were removed during nonstationary conditions, rain, snow, instrument malfunctions, etc. Gaps in the data were not filled. In addition, all computations include only hours with complete original data for both density-based calculations and mixing-ratio-based calculations when actual inputs were available and valid for both methods. For fluxes computed in the traditional manner, the original Webb–Pearman–Leuning correction was used after Webb *et al.* (1980). For fluxes computed using instantaneous mixing ratio, no WPL correction was applied. The AZ-2 site had mixing ratio computed from density during postprocessing, whereas the other eight sites used, direct output of the mixing ratio from the instrument software. Slopes and intercepts of regressions on plots and tables have been analyzed for a statistical significance with 95% confidence level: superscript '*s*' indicates slopes that are significantly different from 1. The absence of a superscript indicates statistically insignificant values.

Table 3 Details of nine field experiments comparing mixing ratio-based flux calculations with traditional density-based flux calculations from the enclosed gas analyzer

Site	Location	Coordinates	Elevation (m)	Ecosystem	Canopy ht (m)	Inst. ht (m)	Average T (°C)	Measurement	
								Start	End
AK	Alaska	65°07′31″N; 147°29′17″W	210	Burned forest	0.5	2.5	12.2	6 August	14 September
AZ-1	Arizona	31°54′30″N; 110°10′22″W	991	Shrubland	0.7	3.6	28.3	5 July	14 July
AZ-2	Arizona	31°82′14″N; 110°86′61″W	1116	Savanna	2.5	6.4	24.7	14 April	29 July
CA-1	California	33°22′38″N; 116°37′22″W	1429	Shrubland	0.7	3.0	17.8	26 May	3 June
CA-2	California	37°04′04″N; 119°11′40″W	2020	Forest	30.0	48.0	21.1	14 July	21 July
NE	Nebraska	40°51′22″N; 96°39′17″W	350	Ryegrass*	0.1	2.6	17.6	15 September	12 November
NM-1	New Mexico	34°21′27″N; 106°41′00″W	1590	Grassland	0.3	2.9	23.7	27 June	5 July
NM-2	New Mexico	34°20′06″N; 104°44′39″W	1593	Shrubland	0.6	2.8	28.0	18 June	25 June
OR	Oregon	44°38′05″N; 123°12′05″W	70	Ag. grassland	0.05	3.0	7.9	5 March	22 March

AK experiment is from UAF site in Alaska. AZ-2 experiment is from USDA site in Arizona. NE experiment is from LI-COR field test facility in Nebraska. The other six experiments are from the AmeriFlux Roving System which conducts intercomparisons of CO_2 and H_2O fluxes and related data among various sites within the AmeriFlux network.
*Data from 2009; the rest in the table are from 2010.

Results and discussion

There are three variables responsible for the difference between the instantaneous gas density and its mixing ratio: (i) instantaneous gas temperature, (ii) instantaneous gas pressure, and (iii) instantaneous water vapor content, as described in Eqn (4). Examining these is important for understanding the way mixing ratio is computed in an enclosed analyzer, for assessing the reliability of such measurements, and ultimately, for confidence in the mixing-ratio-based flux calculations. Of these three variables, the instantaneous water vapor measurements are described in the literature in detail, and are generally well understood. Instantaneous water vapor content in the cell, as a physical variable, has been examined in conjunction with CO_2 for closed-path analyzers utilizing similar technologies for the past 20 years (Leuning & Moncrieff, 1990; Suyker & Verma, 1993), and in the last few years, it was specifically examined for short-tube enclosed analyzers (Clement *et al.*, 2009; Burba *et al.*, 2010). In addition, H_2O measurements in the enclosed analyzer are done at the same rate, within the same volume, and essentially by the same optical and electronic means as the CO_2 measurements (LI-COR Inc, 2010). Reliability of H_2O measurements, resulting CO_2 wet mole fraction, and efficacy of point-by-point conversion to dry mole fraction using instantaneous H_2O was confirmed by a number of closed-path studies and via comparisons with standards (Kowalski & Serrano-Ortiz, 2007; Kowalski, 2008).

Less information is available, or easily deducible, on the instantaneous temperature and the pressure in the cell of an enclosed analyzer, and their effect on the instantaneous mixing ratio. Therefore, we first focus on the instantaneous gas temperature and pressure behavior inside the enclosed analyzer cell, and their implications for the instantaneous mixing ratio computation.

Instantaneous air temperature in the cell

A typical example of 10 Hz air temperature measurements inside the sampling cell of the enclosed analyzer is shown in Fig. 1. Daytime instantaneous air temperature (Fig. 1a) was on average 1.2° warmer than the ambient air, as a result of intentional coupling of the internal electronics and the cell, and also due to the solar load. This design promotes a condensation-free environment inside the sensor, without the need for external heating and resulting increase in power consumption. The instantaneous temperature was significantly attenuated by a 1-m long intake tube in this example (Fig. 1a), and temperature fluctuations in the cell were 20–200 times smaller than that in the ambient conditions outside.

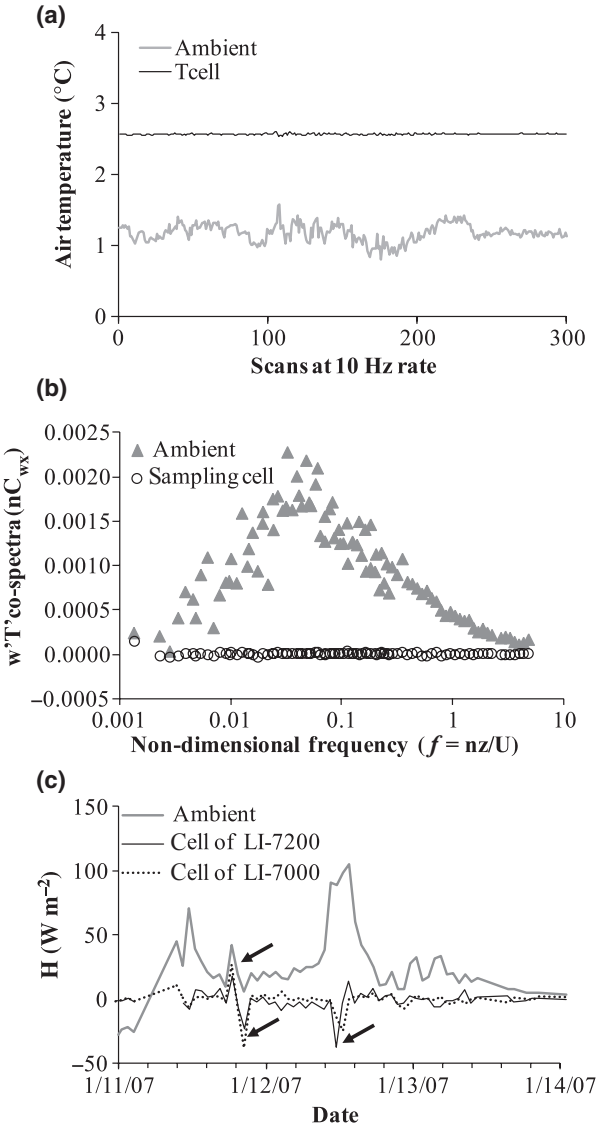

Fig. 1 Fast air temperature inside and outside the enclosed gas analyzer. (a) Example of 30 s of 10 Hz data; (b) ensemble average of 47 daytime hourly co-spectra, not normalized by co-variance to show the absolute magnitudes; (c) H input for WPL temperature term. January 2007, Lincoln, NE Site. Arrows indicate hours when WPL temperature term is not negligible inside the enclosed analyzer with 1-m tube, and inside the traditional closed-path analyzer with 4.5 m tube. Fluctuations in T are small but should be neglected in neither enclosed nor closed-path design. Cell air temperature should be measured at the fast rate to account for this process.

Typical co-spectra of $w'T'$ inside and outside the enclosed analyzer are shown in Fig. 1b. These were not normalized by the mean covariance to better show the influence of the tube attenuation. As with the example of the instantaneous temperature data (Fig. 1a), the co-spectral plot suggests very strong attenuation of the

temperature signal by the intake tube, especially at mid-to-high frequencies. Overall, instantaneous fluctuations were attenuated, on average, by about 90–99% with a 1-m intake tube. Some power still remained at lower frequencies (<0.001), and was not fully attenuated by the intake.

Such significant temperature attenuation minimizes the WPL *H*-term (third member on the right in Eqn 2), but it is important to note that the *H*-term could not be assumed to be negligible in all cases. Figure 1c demonstrates the examples of magnitudes of actual *H* inside the cell of the enclosed analyzer over 3 days with low-to-moderate ambient sensible heat fluxes. The *H* inside the cell was calculated from $w'T'$ using a time delay for CO_2 to demonstrate the size of *H* placed into Eqn (2) when correcting CO_2 flux for WPL terms.

Most of the *H*-term was on the order of a few watts, and could potentially be neglected, especially for summer observances over a green canopy or over wet soil with high $w'q_c'$. However, there were few periods when *H* inside the cell was 10–40 W m^{-2}, translating approximately to a correction of 0.0004–0.002 mmol CO_2 m^{-2} s^{-1}, depending on the concentration of CO_2 and H_2O and sampled air temperature, as follows from the inputs into *H*-term (Eqn 2). This occasional, yet, non-negligible correction probably comes from the low-frequency temperature contributions, as observed in and corroborated by a similar situation with a 4.5-m closed-path analyzer (LI-7000; Fig. 1c).

There are several ways to approach the contribution of the remaining temperature fluctuations in the cell to the fluxes measured with an enclosed gas analyzer:

Using long intake tube and neglecting H-term. This is equivalent to effectively turning an enclosed analyzer into a traditional closed-path analyzer (Table 1). This approach would certainly lead to a reduction in temperature fluctuations beyond 90–99% observed for a 1-m intake tube in most cases, but would come at the expense of increased power consumption, undesirable high frequency losses for CO_2 and more so for H_2O signals (Burba *et al*., 2010), and associated increased uncertainties in H_2O and CO_2 fluxes. In addition, this approach would still be insufficient to correct occasional significant *H*-terms similar to those shown for the closed-path analyzer with a 4.5-m intake tube in Fig. 1c.

Measuring the instantaneous T in the cell and computing H-term from $w'T'$. This approach is based on a traditional WPL equation, which was successfully used for estimating *LE*-term and H-term in open-path analyzers, and for estimating *LE*-term for closed-path analyzers for more than 30 years (Massman, 1991; Leuning, 2004; Lee & Massman, 2011). In an enclosed design, with direct measurements of instantaneous temperature inside the cell, one could use the $w'T'$ to compute *H*-term in the cell, and eliminate temperature effects already significantly minimized by attenuation in the intake tube. However, there are several potential theoretical and methodological issues with this approach. If one uses approach #2 for *H*-term, they would have to consider computing *LE*-term and *P*-term as well. Then, uncertainties in estimating *H* for *H*-term and *E* for *LE*-term using an eddy covariance method would enter the final CO_2 and H_2O flux calculations, and may overpower $w'q_c'$ itself (Eqn 2). There is little consensus on the role and importance of the *P*-term (Lee & Massman, 2011; Nakai *et al*., 2011; Zhang *et al*., 2011, etc.). In addition, it is not fully clear if time delays for the $w'T'$ term would have to be different when computing *H*-term for CO_2 flux vs. those for H_2O flux. It may not be fully clear in which order and at what exact frequency response corrections should be applied to the respective members of *H*-term, *LE*-term, *P*-term, and $w'q_c'$. In addition, several recent studies of closed-path analyzers have shown that computing instantaneous mole fraction point-by-point using instantaneous water vapor measurements may offer advantages over the traditional approach of computing and applying *LE*-term (Leuning, 2004; Kowalski & Serrano-Ortiz, 2007; Leuning, 2007; Kowalski, 2008). The same reasoning should hold for the $w'T'$ and *H*-term.

Measuring instantaneous T in the cell and computing instantaneous mixing ratio. This is a variation of the approach often used for closed-path analyzers using point-by-point correction due to instantaneous water vapor, and assuming instantaneous fluctuations of *T* and *p* are negligible (Ibrom *et al*., 2007). Yet, in the approach proposed in this study, instantaneous *T* and *p* are not neglected but are measured directly. For the specific case of the LI-7200 enclosed analyzer, the point-by-point correction from density to mixing ratio (dry mole fraction) is done in the instrument software in real time without the need for postprocessing.

In this approach, Eqn (1) is used together with Eqn (4) to directly compute the gas flux, and no *H*-term, *LE*-term, or *P*-term is required. This provides a number of advantages, including accounting for small variation in the remaining temperature fluctuations regardless of tube length, for occasional increases in low-frequency contributions resulting in a significant *H*-term, and allowing further shortening of the intake tube, if desired, for specific experiment. In addition, there is no longer a concern about the order of the corrections, separate time delays for CO_2 and H_2O, and the importance, or lack thereof, of the *H*-term in the enclosed or closed-path analyzer.

The flux calculation workflow is reframed from being a fairly complex set of theoretical and methodological problems into a fairly simple engineering task (e.g., measure T fast and well, and at the same time as CO_2 and H_2O). We evaluate the performance of this approach and test it vs. approach #2 in terms of CO_2 and H_2O flux calculations in the respective sections below.

Instantaneous air pressure in the cell

A typical example of 10 Hz air pressure inside the sampling cell of the enclosed analyzer is shown in Fig. 2. Cell air pressure was about 0.4 kPa below ambient (Fig. 2a). A small pressure drop was observed at 14–15 lpm flows, with 0.5 and 1-m intakes fitted with an insect screen and without a filter. Fluctuations in instantaneous cell air pressure were below 0.025 kPa, very close to the ambient, with the use of a flow module without buffer volume (7200-101; LI-COR Biosciences). Similar results were observed with the use of a 20 L buffer between the off-the-shelf industrial pump and the cell (Burba *et al.*, 2010).

Typical co-spectra of $w'p'$ inside and outside the enclosed analyzer are shown in Fig. 2b. The $w'q_c'$ co-spectrum is also provided for reference. The co-spectra were not normalized by the mean covariance to better compare relative magnitudes. As with the instantaneous pressure data (Fig. 2a), the co-spectral plot suggests a very small P-term across all contributing frequencies.

Although pressure variations suggest a minimal P-term (Eqn 3), it is important to note that it is not negligible in all cases. Figure 2c demonstrates the magnitude of the actual $w'p'$ inside the cell of the enclosed analyzer over 3 relatively windy winter days, using the tube without a filter or a rain cup, facing the wind. The $w'p'$ was calculated using a time delay for CO_2 to demonstrate the size of $w'p'$ entered into Eqn (2) when correcting density-based CO_2 flux.

Most of the $w'p'$ was on the order of -0.001 kPa m s^{-1}, and could potentially be neglected. However, there were few periods when $w'p'$ inside cell was -0.004 to -0.005 kPa m s^{-1}, equivalent to the P-term of about 0.0003–0.0006 mmol CO_2 m^{-2} s^{-1}, depending on the concentration of CO_2 and H_2O, and mean pressure (Eqn 3). Such an error may be negligible for normal warm season fluxes, but is on the same order of magnitude as flux itself in winter, and could significantly accumulate over time (Nakai *et al.*, 2011). Similar situations may be expected in closed-path analyzers with long intakes, because p' transits tubes very easily.

As with temperature, there are several ways to account for the contribution of pressure attenuation in the cell to the fluxes measured with an enclosed gas analyzer:

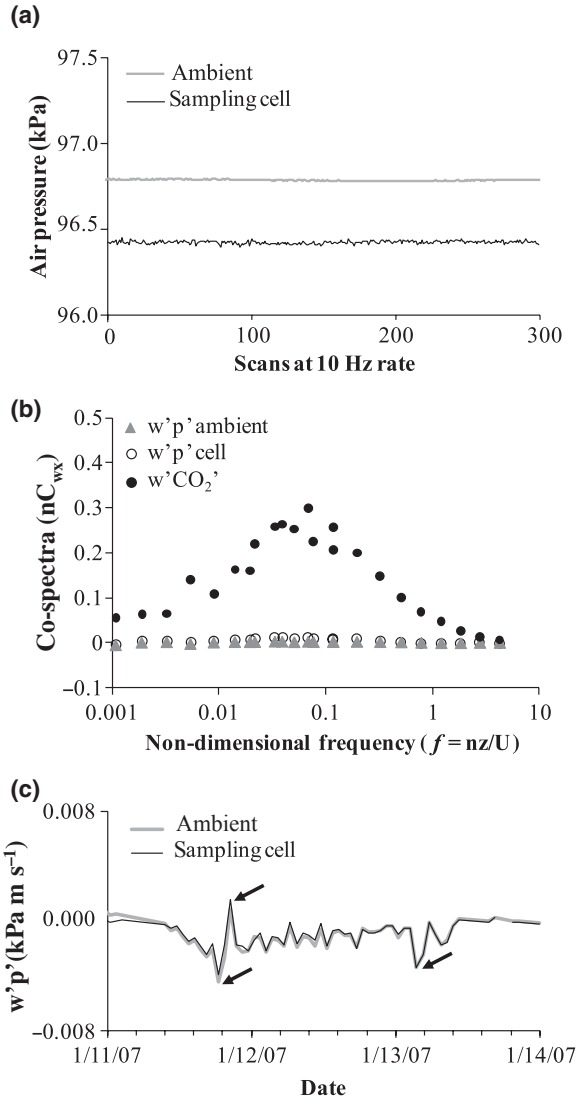

Fig. 2 Fast air pressure inside and outside enclosed gas analyzer. (a) Example of 30 s of 10 Hz data; (b) ensemble average of 47 daytime hourly co-spectra alongside CO_2 flux co-spectra, not normalized by co-variance to show the absolute magnitudes; (c) $w'p'$ input for WPL pressure term. January 2007, Lincoln, NE Site. Arrows indicate hours when temperature term may not be negligible, especially during low gas fluxes. Pressure fluctuations in the cell are small but at times are not negligible. Cell pressure should be measured at the fast rate to account for this process for any tube length, because p' transits tubes very easily.

Neglecting pressure influence and P-term. This has traditionally been done for closed-path and open-path analyzers using either the WPL approach, or using point-by-point conversion to mole fraction. Instantaneous

pressure was not measured in the cell of the analyzers, as it was assumed negligible. However, studies by Massman & Lee (2002), Massman (2004) and Zhang *et al.* (2011) for closed-path and open-path analyzers, and a recent study by Nakai *et al.* (2011) for an enclosed analyzer have demonstrated that the instantaneous pressure fluctuations should not be neglected when computing CO_2 and H_2O fluxes, especially when long-term integration is the focus of the study (Nakai *et al.*, 2011). In addition, this approach would still be insufficient to correct occasional significant *P*-terms similar to those shown in Fig. 2c.

Measuring the instantaneous p in the cell and computing P-term from w'p'. This approach is based on a traditional WPL equation, modified by Massman & Lee (2002) and Nakai *et al.* (2011) to a form which does not neglect *P*-term. This is rarely used in the present flux calculations (Lee & Massman, 2011; Nakai *et al.*, 2011; Zhang *et al.*, 2011). As with temperature, there are few methodological questions about this method. Using approach #2 for *P*-term generally implies computing *LE*-term and *H*-term as well. Then, uncertainties in estimating these terms using respective fluxes measured by eddy covariance method enter the final flux calculations, and may overpower raw $w'q_c'$ itself (Lee & Massman, 2011). At present, there is little consensus on the role and importance of the *P*-term (Lee & Massman, 2011; Nakai *et al.*, 2011; Zhang *et al.*, 2011, etc.). Also, it is not entirely clear if time delays for $w'p'$ would have to be different when computing the *P*-term for CO_2 flux vs. H_2O flux. It may not be fully clear in which order and what exact frequency response corrections and transfer functions should be applied to the members of Eqn (2). In addition, several recent studies of closed-path analyzers have shown that computing instantaneous mole fraction point-by-point using instantaneous water vapor measurements may offer advantages over the traditional approach of computing and applying the *LE*-term (Leuning, 2004; Kowalski & Serrano-Ortiz, 2007; Leuning, 2007; Kowalski, 2008). The same reasoning should hold for the case of $w'p'$ and *P*-term.

Measuring instantaneous p in the cell and computing instantaneous mixing ratio. In this approach, instantaneous *p* is incorporated into Eqn (4), and Eqn (1) is then used to directly compute the gas flux, so that no *P*-term, *H*-term, or *LE*-term is required. As in the case of temperature, this provides a number of advantages, including accounting for small variations in the pressure fluctuations due to wind and pressure fields, pump imperfections, and regardless of occasional high $w'p'$. Also, discussion is no longer required on the importance of the instantaneous pressure fluctuations, on the order of the corrections, or on separate time delays for CO_2 and H_2O in the enclosed or closed-path analyzer.

The flux calculation workflow accounting for the pressure fluctuations is reframed from being an unsettled methodological issue to a fairly simple engineering task (e.g., measure *p* fast and well, at the same time as CO_2 and H_2O). We evaluate the performance of this approach and test it vs. approach #2 in terms of CO_2 and H_2O flux calculations in the respective sections below.

Verification of real-time computation of mixing ratio

The enclosed gas analyzer software uses Eqn (4) with inputs from instantaneous temperature and pressure measurements made in the cell to compute the mixing ratio of CO_2 and H_2O in real time. Programming this process is very difficult, because measurements of CO_2, H_2O, *T*, and *p* have to be done in such a way that an entire air parcel passing through the cell at a specific moment is characterized at that same moment. Such characterization is fairly straightforward for CO_2 and H_2O, as they are measured essentially at the same time and over the same volume. It is a bit more difficult with pressure, as one needs to make sure that electronic delays are set up in such a way that pressure of the air parcel is measured at the same time as CO_2 and H_2O. This is aided by an extremely rapid response of a differential pressure sensor deployed in the cell, and nearly instant propagation of pressure fluctuations from the cell into the pressure sensor. Measuring temperature in the cell requires a more sophisticated approach, as the thermocouple has a finite time delay due to thermal inertia of the junction bid, and because the absolute number and attenuation are different for T_{in} and T_{out}. This implies that characterization of the air parcel over the entire cell requires weighting T_{in} and T_{out} to obtain *T*, and delaying all other signals to match *T* for a given flow rate as described in Materials and methods.

To be confident in the instantaneous mixing ratio data, these complex multistage onboard computations need to be verified by hand calculations during postprocessing, using raw time series for all inputs. This is done to make sure that all delays, weighting, and synchronization are performed in the software correctly. Figure 3a–d shows examples of 10 Hz mixing ratio data for CO_2 and H_2O computed in real time inside the instrument and computed from 10 Hz density data by hand using MS-Excel spreadsheet. In all cases, mixing ratio computed in real time inside the instrument was virtually identical to that computed manually. Slight noise in the data in Fig. 3b is related to rounding errors in the manual calculations in conjunction with the narrow range (<1.1 ppm) of the sampled CO_2 concentrations.

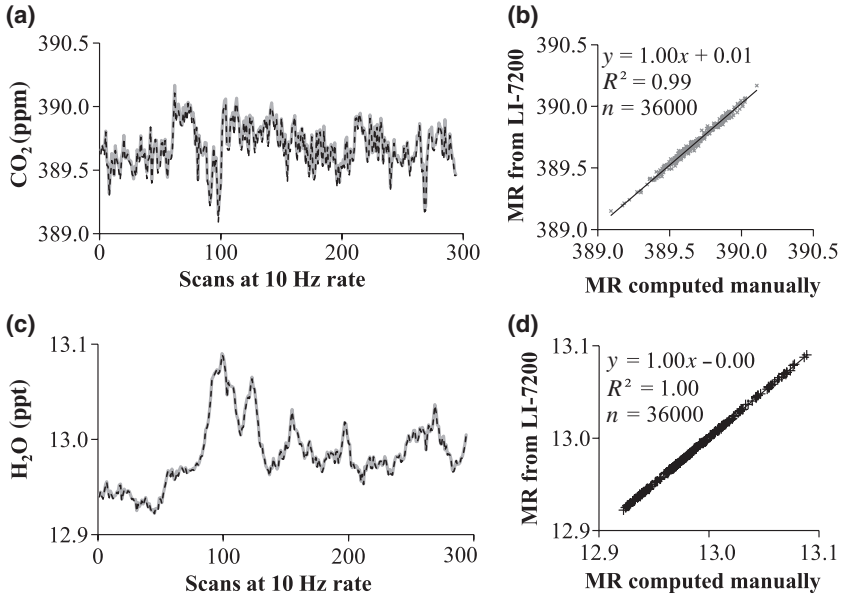

Fig. 3 Example of 10 Hz mixing ratio data from the enclosed gas analyzer computed in real time inside the instrument (solid gray line) plotted vs. those computed from 10 Hz density data by hand (dotted black line): (a) example of 30 s of CO_2 data plotted vs. time; (b) 1 h of 10 Hz CO_2 data computed by the instrument vs. those computed by hand; (c) example of 30 s of H_2O data plotted vs. time; (d) 1 h of 10 Hz H_2O data computed by the instrument vs. those computed by hand. November 12, 2009, 13:00–14:00 hours, Lincoln, NE Site. Instrument software computes mixing ratio well for both CO_2 and H_2O.

No visual or statistical difference was found between automated and manual calculations in other randomly chosen periods during this and other experiments, and for different output venues (e.g., Ethernet, USB, SDM, Serial, Analog). The results confirm that mixing ratio can be computed correctly in real time using instantaneous measurements of temperature and pressure in the enclosed analyzer with a short intake tube.

Comparison of mixing ratio-based and density-based hourly fluxes

With properly computed instantaneous mixing ratio, hourly fluxes without WPL terms (Eqn 1) should be very similar or identical to those computed using the traditional approach (Eqn 2), with the WPL correction. Figure 4a demonstrates an example of the similarity for

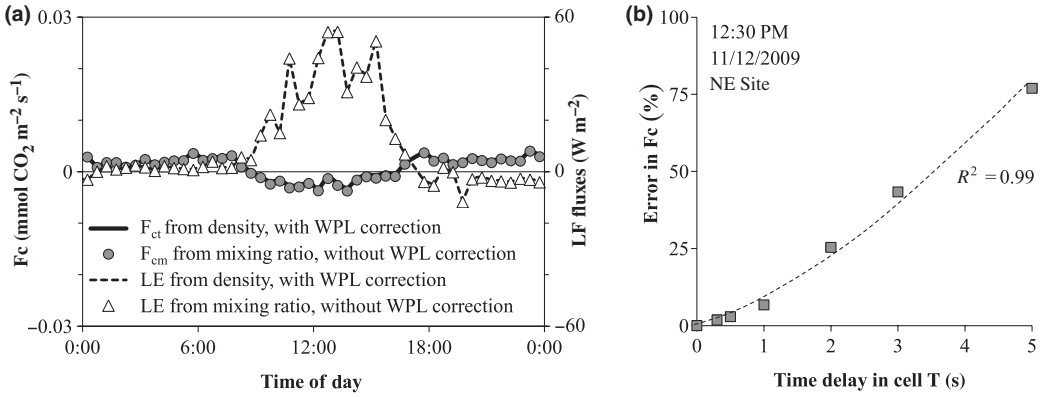

Fig. 4 Examples of (a) diurnal CO_2 and H_2O fluxes computed from mixing ratio without WPL correction and computed from traditional density-based fluxes with WPL correction; and (b) potential errors in mixing ratio-based flux calculations that could have occurred if cell temperature was not properly delayed in the instrument in relation to other signals required for instantaneous conversion from density to mixing ratio following Eqn 4. November 12, 2009, Lincoln, NE Site. When instantaneous inputs in Eqn 4 are intentionally misaligned, the error in the mixing ratio-based fluxes rapidly increases with the delay. When the inputs are properly synchronized, as computed by the instrument software in real time, the mixing ratio-based fluxes match density-based fluxes.

the hourly fluxes over 1 day during the experiment in Nebraska (NE in Table 3). Very little difference is observed between mixing ratio-based flux calculations and traditional density-based flux calculations for both CO_2 and H_2O during day and night, and for positive and negative flux values.

However, the similarity of mixing ratio-based and density-based flux calculations from the same enclosed instrument should not be taken for granted. Using the traditional approach (Eqn 2), *H* and *E* are computed during the postprocessing, and proper delays are determined using circular correlation or other similar means. So, if the relevant instantaneous time series (e.g., CO_2, H_2O, *T*, *P*) were to be misaligned in relation to each other, the postprocessing routine would re-align them, leading to correct results for the traditional flux calculations. Using the mixing ratio-based approach (Eqn 1) with the instantaneous mixing ratio output (Eqn 4), there is no opportunity for on-the-fly postprocessing to re-align the misaligned time series used in Eqn (4). Hence, the instrument must be designed such that the relevant time series are properly aligned and synchronized with each other at high speed. Figure 4b illustrates the importance of such alignment using cell temperature as an example. When instantaneous cell *T* was intentionally misaligned, the error in the mixing ratio-based CO_2 fluxes rapidly increased with the delay. Daytime CO_2 uptake becomes larger as if it was under-corrected by *H*-term in WPL. Sub-second delays caused errors of few percent, and multi-second delays caused flux errors as high as 25–75%. When the inputs were properly synchronized, as computed by the instrument software in real time, the mixing ratio-based fluxes matched density-based fluxes, as expected from the theory.

This example also emphasizes that to confidently use the mixing ratio-based approach and benefit from its advantages, the enclosed design needs to be tested in a wide range of conditions to make sure that it is capable of consistently producing mixing ratio-based fluxes comparable to the traditional density-based fluxes.

Figure 5 shows one-to-one comparison of hourly CO_2 fluxes from nine experiments conducted over broad range of geographic and climatic conditions with various experimental setups (Table 3) for the entire duration of each respective experiment. Table 4 summarizes the slopes, offsets, and R^2 for each experiment. In all cases, the fluxes measured using mixing ratio were within 4% of those measured in a traditional manner using density-based covariance and WPL corrections, with six of nine sites being within 2%. The largest difference of 4% was observed only at the CA-2 site, which had a measurement height of 7–18 times taller than any other site, the highest H_2O flux affecting *LE*-term in WPL, and the fewest number of available hours of data. Considering the error bars of the eddy covariance

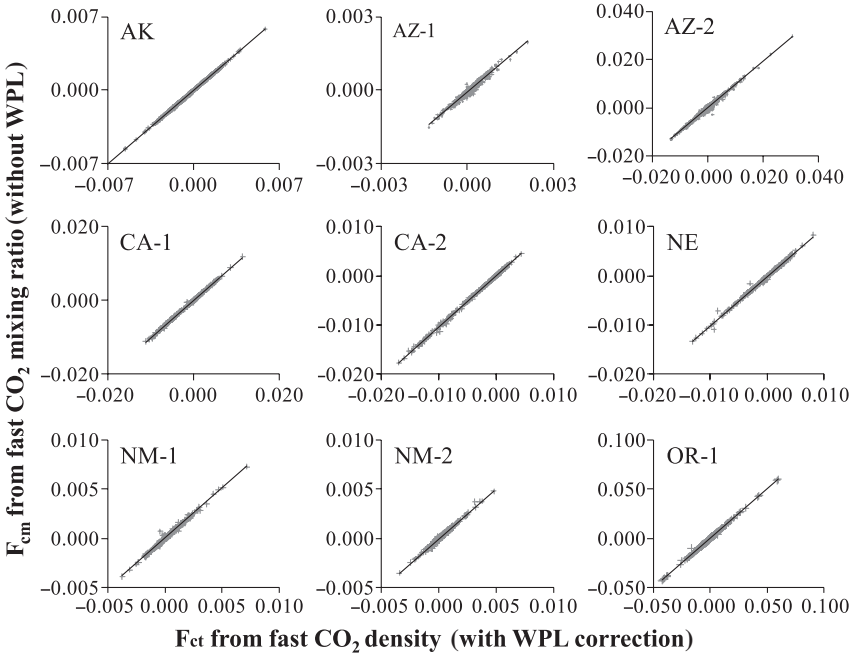

Fig. 5 Mixing ratio-based CO_2 fluxes without WPL correction plotted vs. traditional density-based fluxes at nine different deployments over a wide range of environmental conditions, in mmol CO_2 m^{-2} s^{-1}. Mixing ratio-based approach performs well for CO_2 flux across all sites collectively (Table 4), and for nearly each hour at each site.

Table 4 Results of CO_2 flux comparisons between mixing ratio-based flux calculations and traditional density-based flux calculations from the enclosed gas analyzer: [mixing ratio-based fluxes] = [slope] × [traditional density-based fluxes] + [offset]

Site	Slope	Offset (mmol m^{-2} s^{-1})	R^2	n (h)
AK	1.00	−0.0009	1.00	1897
AZ-1	1.00	−0.00007	0.96	441
AZ-2	0.97	−0.00003	0.99	5828
CA-1	1.02	0.00003	1.00	381
CA-2	1.04[s]	0.00001	1.00	318
NE	1.00	−0.00006	1.00	370
NM-1	1.03[s]	−0.00004	0.99	381
NM-2	1.02	−0.00006	0.99	346
OR	1.01	−0.00001	1.00	806
All data	1.01	−0.00013	0.99	8869

Table 5 Results of H_2O flux comparisons between mixing ratio-based flux calculations and traditional density-based flux calculations from the enclosed gas analyzer: [mixing ratio-based fluxes] = [slope] × [traditional density-based fluxes] + [offset]

Site	Slope	Offset (W m^{-2})	R^2	n (h)
AK	1.00	0.0	1.00	1897
AZ-1	1.00	0.0	1.00	441
AZ-2	1.00	0.0	1.00	5828
CA-1	1.01	0.0	1.00	381
CA-2	1.01	−0.1	1.00	318
NE	1.01	−0.1	1.00	370
NM-1	1.01	−0.1	1.00	381
NM-2	1.01	0.0	1.00	346
OR	1.01	0.0	1.00	806
All data	1.01	0.0	1.00	8869

measurements to be on the order of 10–20% (Goulden *et al.*, 1996; Richardson *et al.*, 2006; Billesbach, 2011), hourly mixing ratio-based fluxes at all sites were nearly identical to the traditional density-based fluxes. Water vapor fluxes were within 1% at all nine sites (Fig. 6; Table 5), as expected due to a much larger raw covariance flux dominating the WPL corrections.

On average, mixing ratio-based fluxes of CO_2 and H_2O from all nine sites were about 1% larger (ns) than density-based fluxes, with negligible offsets. No specific connection was found between site setup or weather parameters, and between the small differences observed between mixing-ratio-based and density-based fluxes. It is also important to note that in the case

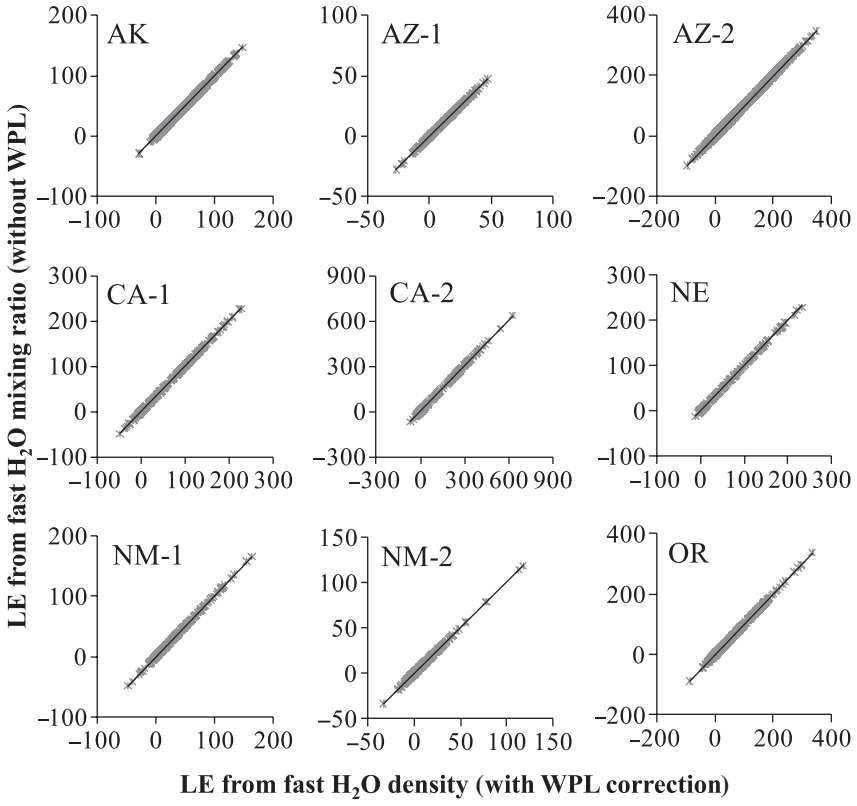

Fig. 6 Mixing ratio-based H_2O fluxes (LE) without WPL correction plotted vs. traditional density-based fluxes with WPL correction at nine different deployments over a wide range of environmental conditions, W m^{-2}. Mixing ratio-based approach performs well for H_2O flux across all sites collectively (Table 5), and for each hour at each site.

of H_2O fluxes, this statistically insignificant 1% would imply ca. 2–4% improvement in the energy budget closure, depending on the size of the available energy, although this is a small improvement of the average imbalance of about 20% among sites (Wilson *et al.*, 2002).

The consistent results across a wide range of conditions suggest that using instantaneous mixing ratio to compute hourly fluxes of CO_2 and H_2O, without WPL correction, is in no way inferior to the traditional way of computing fluxes from densities and applying WPL corrections in postprocessing. However, the use of the mixing ratio may be more beneficial than the traditional method in terms of methodology, because it eliminates several areas of little consensus in the community related to data processing, namely:

1 Order of the frequency response corrections in relation to WPL corrections (Massman, 2004).
2 Necessity, or lack thereof, of using separate time delays for T and H_2O when computing H and E for input into WPL terms in Eqn (2) (Ibrom *et al.*, 2007).
3 Necessity, or lack thereof, of including pressure term in WPL equation (Lee & Massman, 2011; Nakai *et al.*, 2011; Zhang *et al.*, 2011).
4 The form of the WPL equation itself (Liu, 2005; Kowalski, 2006; Liu, 2006; Leuning, 2007; Liu, 2009; Lee & Massman, 2011).

Use of the instantaneous mixing ratio also significantly simplifies the related portion of flux processing down to two essential steps:

1 Running time delay between w' and s' to obtain maximum covariance.
2 Applying frequency response corrections to obtain the final flux.

Another potential upside of mixing ratio-based flux calculations is eliminating uncertainty in eddy flux inputs for *LE*-term and *H*-term (Eqn 2), in favor of introducing the uncertainties from T and p measurements in Eqns (1) and (4). Approximate uncertainties for eddy covariance-based E and H in WPL equation would be 10–20% (Goulden *et al.*, 1996; Richardson *et al.*, 2006; Billesbach, 2011), whereas uncertainty associated with T and p measurements would be on the order of single digit percentages or less depending on ambient conditions and instrument setup and maintenance.

The findings presented in this study also validate recent findings and recommendations on using mixing ratio and mole fraction without WPL correction in the literature from closed-path analyzers (Ibrom *et al.*, 2007; Kowalski & Serrano-Ortiz, 2007; Leuning, 2007; Kowalski, 2008) and enclosed analyzers (Nakai *et al.*, 2011), and may help to substantially unify data processing steps in the flux network and to assure better intercomparisons between sites and networks.

All evidence from this and other studies points to the mixing ratio being either similar or superior to a traditional density-based way of computing fluxes, and no evidence points to the mixing ratio being inferior to a density-based approach. However, the question as to which of the two approaches produces a better measure of eddy flux could only be resolved conclusively via a direct experiment over the area with known flux magnitudes, similar to parking lot experiments conducted by Ham & Heilman (2003), Ono *et al.* (2008), Kondo and Tsukamoto (2008) designed to verify the performance of WPL approach. However, in the case of an enclosed gas analyzer with instantaneous mixing ratio output, the parking lot experiment may need to be conducted over a wet lot to maximize the *LE*-term in the WPL correction. In such an experiment, the nearness of CO_2 flux to zero would be an ultimate criterion in determining which approach is better. Such an experiment would also help to define flux uncertainty and minimum detectable flux for the mixing ratio-based approach in comparison with the traditional density-based approach.

Conclusions

A newly designed enclosed gas analyzer measures instantaneous temperature and pressure in the cell, simultaneously with CO_2 and H_2O, so that instantaneous gas density and mixing ratio can be output at the same time. The performance of the new design was examined over a wide range of conditions using data from nine field experiments. Following are the five key conclusions:

1 Temperature attenuation in a 1-m intake tube is 90–99%. The remaining *H*-term in WPL correction is small but not negligible, nor it is always negligible in a traditional closed-path design with 4.5 m tube. The *H*-term should be considered in all cases using fast temperature measured inside the cell. *H*-term can be accounted for explicitly after Webb *et al.* (1980) or implicitly using instantaneous mixing ratio output from the enclosed analyzer.

2 Pressure fluctuations in the enclosed design are small, and the *P*-term in the WPL correction is close to zero but not negligible, nor is it always negligible in a traditional closed-path design. The *P*-term should be accounted for in all cases by measuring fast pressure inside the cell. This can be done explicitly by computing the *P*-term after Lee & Massman

(2011) or implicitly using instantaneous mixing ratio output from the enclosed analyzer.

3 Mixing ratio output from the enclosed analyzer, incorporating water dilution and pressure–temperature expansions and contractions, can be computed in real time in the instrument software, so that no point-by-point conversion from density is needed in postprocessing.

4 Using the instantaneous mixing ratio for calculations of hourly fluxes, without WPL corrections, results in fluxes nearly identical to the traditional density-based fluxes with subsequent WPL corrections across all experiments over a wide range of conditions.

5 While consistent results across a wide range of conditions suggest that the mixing ratio approach is similar to the traditional approach in terms of the hourly flux magnitudes, the mixing ratio may be superior methodologically, because:

- it eliminates several areas of controversy in the community related to data processing (e.g., order of the corrections; time delay issues for T and H_2O when computing H and E for the WPL; pressure term inclusion in WPL; the form of the WPL itself, etc.);
- it significantly simplifies the related portion of flux processing down to two steps (determining time delay between w' and s' and applying frequency corrections);
- it reframes the flux calculation workflow from being a fairly complex theoretical and methodological problem to a fairly simple engineering task (e.g., measure T and p fast and well, at the same time as CO_2 and H_2O);
- it potentially could increase flux data quality and temporal resolution, and reduce the size of uncertainty and minimum detectable flux, because errors in *LE*-term, *H*-term, and *P*-term coming from eddy covariance (±10% to ±20%) are replaced with errors from H_2O, T, and p measurements in the cell (less than a few single percentages);
- it may help to substantially unify data processing steps in the flux community and to assure better intercomparison between different sites and networks.

Acknowledgements

We are very grateful to research groups and individuals who tested early prototypes of the LI-7200, and suggested important additions and improvements to its design. In particular, we thank the US Department of Energy Biological and Environmental Research, Terrestrial Carbon Program (grant no. DE-FG02-06ER6430) for support of the AmeriFlux QA intercomparisons and AmeriFlux research and synthesis. We thank Drs Nicola Arriga, Andrew Black, Christian Bruemmer, Robert Clement, John Grace, Steve Oberbauer, Dario Papale, Jessica Schedlbauer, and Mrs. Zoran Nesic and Dominic Lessard. We also thank the Principal Investigators of the six sites where the AmeriFlux Intercomparison System was positioned, Drs Michael Goulden, Marcy Litvak, Walter Oechel, and Shirley Papuga. The authors deeply appreciate support provided by LI-COR LI-7200 team, and thank Ron Nelson for proofreading the manuscript. We also are very grateful to Drs B. Gioli, L. Gu, R. Leuning, W. Massman, A. Suyker, and D. Zona for important discussions related to mixing ratio-based flux calculations.

References

Aubinet M, Grelle A, Ibrom A *et al*. (1999) Estimates of the annual net carbon and water exchange of forests: the EUROFLUX methodology. In: *Advances in Ecological Research* (eds Fitter A, Raffaelli D), pp. 113–175. Academic Press, San Diego, USA.

Billesbach DP (2011) Estimating uncertainties in individual eddy covariance flux measurements: a comparison of methods and a proposed new method. *Agricultural and Forest Meteorology*, **151**, 394–405.

Burba G, McDermitt D, Grelle A, Anderson D, Xu L (2008) Addressing the influence of instrument surface heat exchange on the measurements of CO_2 flux from open-path gas analyzers. *Global Change Biology*, **14**, 1854–1876.

Burba G, McDermitt DK, Anderson DJ, Furtaw MD, Eckles RD (2010) Novel design of an enclosed CO_2/H_2O gas analyser for eddy covariance flux measurements. *Tellus B*, **62**, 743–748.

Clement RJ, Burba GG, Grelle A, Anderson DJ, Moncrieff JB (2009) Improved trace gas flux estimation through IRGA sampling optimization. *Agricultural and Forest Meteorology*, **149**, 623–638.

Foken T, Gockede M, Mauder M, Mahrt L, Amiro B, Munger J (2004) Post-field data quality control. In: *Handbook of Micrometeorology: A Guide for Surface Flux Measurements* (eds Lee X, Massman W, Law B), pp. 81–108. Kluwer Academic Publishers, Dordrecht.

Goulden ML, Munger JW, Fan S-M, Daube BC, Wofsy SC (1996) Measurements of carbon sequestration by long-term eddy covariance: methods and a critical evaluation of accuracy. *Global Change Biology*, **2**, 169–182.

Grelle A, Burba G (2007) Fine-wire thermometer to correct CO_2 fluxes by open-path analyzers for artificial density fluctuations. *Agricultural and Forest Meteorology*, **147**, 48–57.

Ham J, Heilman JL (2003) Experimental test of density and energy-balance corrections on carbon dioxide flux as measured using open-path eddy covariance. *Agronomy Journal*, **95**, 1393–1403.

Ibrom A, Dellwik E, Larsen SE, Pilegaard KIM (2007) On the use of the Webb–Pearman–Leuning theory for closed-path eddy correlation measurements. *Tellus B*, **59**, 937–946.

Jarvi L, Mammarella I, Eugster W *et al.* (2009) Comparison of net CO_2 fluxes measured with open and closed path infrared gas analyzers in urban complex environment. *Boreal Environmental Research*, **14**, 499–514.

Kaimal JC, Wyngaard JC, Izumi Y, Coté OR (1972) Spectral characteristics of surface-layer turbulence. *Quarterly Journal of the Royal Meteorological Society*, **98**, 563–589.

Kondo F, Tsukamoto O (2008) Evaluation of webb correction on CO_2 flux by eddy covariance technique using open-path gas analyzer over asphalt surface. *Journal of Agricultural Meteorology*, **64**, 1–8.

Kowalski A (2006) Comment on "An Alternative Approach for CO_2; Flux Correction Caused by Heat and Water Vapour Transfer" by Liu. *Boundary-Layer Meteorology*, **120**, 353–355.

Kowalski AS (2008) Comment on "The Storage Term in Eddy Flux Calculations". *Agricultural and Forest Meteorology*, **148**, 691–692.

Kowalski A, Serrano-Ortiz P (2007) On the relationship between the eddy covariance, the turbulent flux, and surface exchange for a trace gas such as CO_2. *Boundary-Layer Meteorology*, **124**, 129–141.

Law BE (2006) Carbon dynamics in response to climate and disturbance: recent progress from multi-scale measurements and modeling in AmeriFlux. In: *Plant Responses to Air Pollution and Global Change*. (ed. Yamamoto S), pp. 205–213. Springer, Tokyo, Japan.

Lee X, Massman W (2011) A perspective on thirty years of the Webb, Pearman and Leuning density corrections. *Boundary-Layer Meteorology*, **139**, 37–59.

Lenschow DH, Raupach MR (1991) The attenuation of fluctuations in scalar concentrations through sampling tubes. *Journal of Geophysical Research*, **96**, 15259.

Leuning R (2004) Measurements of trace gas fluxes in the atmosphere using eddy covariance: WPL calculations revisited. In: *Handbook of Micrometeorology: A Guide for Surface Flux Measurements and Analysis*, Vol 23 (eds Lee X, Massman WJ, Law B), pp. 119–131. Kluwer Academic Publishers, Dordrecht, the Netherlands.

Leuning R (2007) The correct form of the Webb, Pearman and Leuning equation for eddy fluxes of trace gases in steady and non-steady state, horizontally homogeneous flows. *Boundary-Layer Meteorology*, **123**, 263–267.

Leuning R, Judd MJ (1996) The relative merits of open- and closed-path analysers for measurement of eddy fluxes. *Global Change Biology*, **2**, 241–253.

Leuning R, Moncrieff J (1990) Eddy-covariance CO_2 flux measurements using open- and closed-path CO_2 analysers: corrections for analyser water vapour sensitivity and damping of fluctuations in air sampling tubes. *Boundary-Layer Meteorology*, **53**, 63–76.

LI-COR, Inc (2001) *LI-7500 CO_2/H_2O Open Path Instruction Manual*. LI-COR Inc., Lincoln, NE.

LI-COR, Inc (2010) *LI-7200 CO_2/H_2O Instruction Manual*. LI-COR Inc., Lincoln, NE.

Liu H (2005) An alternative approach for CO_2: flux correction caused by heat and water vapour transfer. *Boundary-Layer Meteorology*, **115**, 151–168.

Liu H (2006) Reply to the Comment by Kowalski on "An Alternative Approach for CO_2; Flux Correction Caused by Heat and Water Vapour Transfer". *Boundary-Layer Meteorology*, **120**, 357–363.

Liu H (2009) A re-examination of density effects in eddy covariance measurements of CO_2; fluxes. *Advances in Atmospheric Sciences*, **26**, 9–16.

Massman WJ (1991) The attenuation of concentration fluctuations in turbulent flow through a tube. *Journal of Geophysical Research*, **96**, 15269–15273.

Massman WJ (2000) A simple method for estimating frequency response corrections for eddy covariance systems. *Agricultural and Forest Meteorology*, **104**, 185–198.

Massman WJ (2001) Reply to comment by Rannik on "A simple method for estimating frequency response corrections for eddy covariance systems". *Agricultural and Forest Meteorology*, **107**, 247–251.

Massman WJ (2004) Concerning the measurements of atmospheric trace gas fluxes with open- and closed-path eddy covariance system: the WPL terms and spectral attenuation. In: *Handbook of Micrometeorology: A Guide for Surface Flux Measurement and Analysis*, Vol 29 (eds Lee X, Massman WJ, Law B), pp. 133–158. Kluwer ademic Publishers, Dordrecht.

Massman WJ, Ibrom A (2008) Attenuation of concentration fluctuations of water vapor and other trace gases in turbulent tube flow. *Atmospheric Chemistry and Physics*, **8**, 6245–6259.

Massman WJ, Lee X (2002) Eddy covariance flux corrections and uncertainties in long-term studies of carbon and energy exchanges. *Agricultural and Forest Meteorology*, **113**, 121–144.

Massman W, Lee X, Law BE (eds) (2004). *Handbook of Micrometeorology. A Guide for Surface Flux Measurements and Analysis*. Kluwer Academic Publishers, Boston.

Moore CJ (1986) Frequency response corrections for eddy correlation systems. *Boundary-Layer Meteorology*, **37**, 17–35.

Nakai T, Iwata H, Harazono Y (2011) Importance of mixing ratio for a long-term CO_2 flux measurement with a closed-path system. *Tellus B*, **63**, 302–308.

Ono K, Miyata A, Yamada T (2008) Apparent downward CO_2 flux observed with open-path eddy covariance over a non-vegetated surface. *Theoretical and Applied Climatology*, **92**, 195–208.

Richardson AD, Hollinger DY, Burba GG *et al*. (2006) A multi-site analysis of random error in tower-based measurements of carbon and energy fluxes. *Agricultural and Forest Meteorology*, **136**, 1–18.

Suyker AE, Verma SB (1993) Eddy correlation measurement of CO_2 flux using a closed-path sensor: theory and field tests against an open-path sensor. *Boundary-Layer Meteorology*, **64**, 391–407.

Webb EK, Pearman GI, Leuning R (1980) Correction of flux measurements for density effects due to heat and water vapour transfer. *Quarterly Journal of the Royal Meteorological Society*, **106**, 85–100.

Wilson KB, Goldstein AH, Falge E *et al*. (2002) Energy balance closure at FLUXNET sites. *Agricultural and Forest Meteorology*, **113**, 223–243.

Zhang J, Lee X, Song G, Han S (2011) Pressure correction to the long-term measurement of carbon dioxide flux. *Agricultural and Forest Meteorology*, **151**, 70–77.